 CMES, vol.9, no.1, pp.49-55, 2005

Elastic waves in a hybrid multilayered piezoelectric plate

X. Han[1], H. Ding*[2], and G. R. Liu[1]

Abstract: An analytical-numerical method is presented for analyzing dispersion and characteristic surface of waves in a hybrid multilayered piezoelectric plate. In this method, the multilayered piezoelectric plate is divided into a number of layered elements with three-nodal-lines in the wall thickness, the coupling between the elastic field and the electric field is considered in each element. The associated frequency dispersion equation is developed and the phase velocity and slowness, as well as the group velocity and slowness are established in terms of the Rayleigh quotient. Six characteristic wave surfaces are introduced to visualize the effects of anisotropy and piezoelectricity on wave propagation. Examples provide a full understanding for the complex phenomena of elastic waves in hybrid multilayered piezoelectric media.

keyword: Smart materials, Piezoelectric, Elastic waves

1 Introduction

The studies on wave propagation in piezoelectric media are essential for the application of piezoelectric materials, such as the design and manufacture of the ultrasonic piezoelectric motor. Wave propagation and vibration in pure piezoelectric media have been reported. Bleustein (1969) gave some models of wave propagation in infinite piezoelectric plates. Curtis and Redwood (1973) studied the transverse surface waves in piezoelectric materials. Sun and Cheng (1974) investigated the acoustic surface waves in a piezoelectric cylinder with metallic overlay. Investigations have been also undertaken for the characteristic analysis of various waves in piezoelectric media. The references listed herein (Pauley and Dong, 1976; Lewis, 1985; Shiosai, 1986; Toda and Mizutain, 1988; Honein et al., 1991; Liu and Tani1994Siao and Dong, 1994; Zhang et al., 1998; Adler, 2000; Gopinathan et al., 2000; Vel and Batra, 2001; Wang, 2001; Liu H et al., 2002; Liu et al., 2003; Han and Liu, 2003; Han et al., 2004; Liu and Wang, 2005) are some examples of the contributions in this area.

To visualize the effects of anisotropy on wave propagation, Liu et al. (1991) and Liu and Xi (2001) introduced a set of six characteristic wave surfaces for composite laminates: phase velocity surface (PVS), phase slowness surface (PSS), phase wave surface (PWS), group velocity surface (GVS), group slowness surface (GSS) and group wave surface (GWS). This paper attempts to explore such unique and important wave properties of hybrid multilayered piezoelectric plates, and to clear visualize the dispersion behavior and characteristics of wave surface. In the investigation, the laminated plate is divided into layered elements with three-nodal-lines along the wall thickness. The Hamilton principle is used to develop the dispersion equations, then the phase velocity and slowness as well as the group velocity and slowness are established in terms of the Rayleigh quotient. The effects of piezoelectricity, the wave propagation modes, and the frequency and group velocity dispersion behaviors as well as characteristic wave surfaces are discussed via numerical examples.

2 Basic equation

Consider a hybrid multilayered piezoelectric plate with thickness H as shown in Fig. 1. The constitutive relations expressing the coupling between the elastic field and the electric field can be written as:

$$\begin{aligned} \boldsymbol{\sigma} &= \mathbf{c}\boldsymbol{\varepsilon} - \mathbf{e}^{\mathrm{T}}\mathbf{E} \\ \mathbf{D} &= \mathbf{e}\boldsymbol{\varepsilon} + \mathbf{g}\mathbf{E} \end{aligned} \tag{1}$$

where $\boldsymbol{\sigma}$ is stress tensor, $\boldsymbol{\varepsilon}$ strain tensor, $\mathbf{D}$ electric displacement vector, and $\mathbf{E}$ electric field vector, $\mathbf{c}$, $\mathbf{e}$ and $\mathbf{g}$ are the elastic, piezoelectric and dielectric material matrices, respectively.

[1] College of Mechanical & Automotive Engineering, Hunan University, Changsha 410082, P. R. China, hanxu@hnu.cn

[2] Corresponding author, Institute of Mechanics, CAS 15 Northwest road of 4th Round, Haidian Beijing 100080, P. R. China, Hding@imech.as.cn

The electrical field **E** is related to the electrical potential φ by

$$\mathbf{E} = -grad\varphi \tag{2}$$

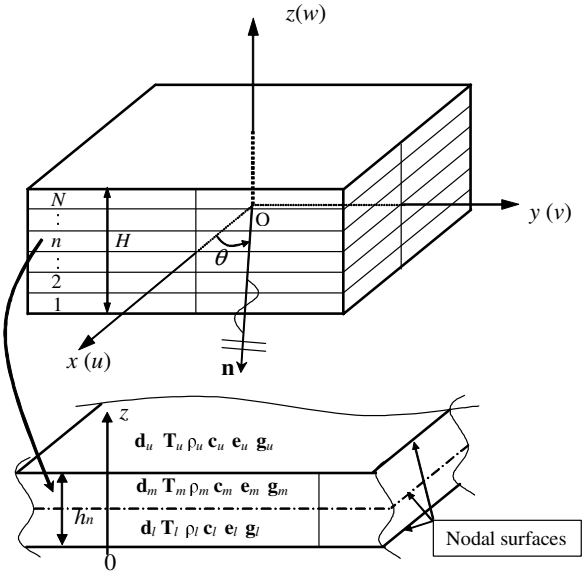

Figure 1 : A hybrid multilayered piezoelectric plate and its *n*th isolated layer element

and the mechanical strain **ε** to the mechanical displacement **U** by

$$\boldsymbol{\varepsilon} = \mathbf{L}_d\mathbf{U} \tag{3}$$

where $\mathbf{L}_d$ is the differential operator matrix and can be written as

$$\mathbf{L}_d^T = \begin{bmatrix} \frac{\partial}{\partial x} & 0 & 0 & 0 & \frac{\partial}{\partial z} & \frac{\partial}{\partial y} \\ 0 & \frac{\partial}{\partial y} & 0 & \frac{\partial}{\partial z} & 0 & \frac{\partial}{\partial x} \\ 0 & 0 & \frac{\partial}{\partial z} & \frac{\partial}{\partial y} & \frac{\partial}{\partial x} & 0 \end{bmatrix} \tag{4}$$

or

$$\mathbf{L}_d = \mathbf{L}_{dx}\frac{\partial}{\partial x} + \mathbf{L}_{dy}\frac{\partial}{\partial y} + \mathbf{L}_{dz}\frac{\partial}{\partial z} \tag{5}$$

where $\mathbf{L}_{dx}$, $\mathbf{L}_{dy}$ and $\mathbf{L}_{dz}$ are also (6×3) matrices and can be obtained by inspection of Eq. (5).

The electric behaviour is described by Maxwell's equation considering that the piezoelectric media are insulating:

$$div\mathbf{D} = 0 \tag{6}$$

3 Formulation

Suppose that the hybrid multilayered piezoelectric plate is subdivided into N layered elements in the thickness direction, the thickness of the nth element is denoted by h_n. The mass density, elastic coefficient matrix, piezoelectric and dielectric material constant matrices on the lower, middle and upper surface of the nth element are denoted by ρ_n, $\mathbf{c}_n = (c_{ij})_n\ (i,j=1,...,6)$, $\mathbf{e}_n = (e_{ij})_n\ (i=1,2,3;\ j=1,...,6)$, $\mathbf{g}_n = (g_{ij})_n\ (i,j=1,2,3)$, respectively.

Approximating the displacement **U** and electric static potential **φ** within an element as

$$\mathbf{U}(x,y,z,t) = \mathbf{N}_d(z)\mathbf{d}(x,y,t) \tag{7}$$

$$\boldsymbol{\varphi}(x,y,z,t) = \mathbf{N}_\phi(z)\boldsymbol{\phi}(x,y,t) \tag{8}$$

where **d** and **ϕ** are nodal displacement and nodal electric potential vectors,

$$\mathbf{d}^T = \{\mathbf{d}_l^T\ \ \mathbf{d}_m^T\ \ \mathbf{d}_u^T\} \tag{9}$$

$$\boldsymbol{\varphi}^T = \{\boldsymbol{\varphi}_l^T\ \ \boldsymbol{\varphi}_m^T\ \ \boldsymbol{\varphi}_u^T\}$$

in which $\mathbf{d}_i^T = \{u\ \ v\ \ w\}_i\ (i=l,m,u)$.

$\mathbf{N}_d$and $\mathbf{N}_\phi$ in Eqs. (7) and (8) are the respective shape function matrices given by

$$\mathbf{N}_d = [(1-3\overline{z}+2\overline{z}^2)\mathbf{I}4(\overline{z}-\overline{z}^2)\mathbf{I}(2\overline{z}^2-\overline{z})\mathbf{I}] \tag{10}$$

$$\mathbf{N}_\phi = [(1-3\overline{z}+2\overline{z}^2)4(\overline{z}-\overline{z}^2)(2\overline{z}^2-\overline{z})] \tag{11}$$

in which $\overline{z} = z/h_n$, and **I** is a 3×3 identity matrix.

The governing equations of the nth element may be developed by means of Hamilton's principle,

$$\delta\int Ldt = 0 \tag{12}$$

in which δ denotes the first order variation and Lagrangian term L is determined by

$$L = E_k - E_s + E_d + W \tag{13}$$

with Elastic energy E_s

$$E_s = \frac{1}{2}\int_0^{h_n} \boldsymbol{\varepsilon}^T\boldsymbol{\sigma}dz \tag{14}$$

and Dielectric energy E_d

$$E_d = \frac{1}{2}\int_0^{h_n} \mathbf{E}^T\mathbf{D}dz \tag{15}$$

and Kinetic energy E_k

$$E_k = \frac{1}{2}\int_0^{h_n} \rho_n \mathbf{U}^T \ddot{\mathbf{U}} dz \tag{16}$$

where the superscript T denotes the transposed matrix. W is generated by external mechanical or electrical excitation with the form of

$$W = \mathbf{d}^T \mathbf{F} + \boldsymbol{\phi}^T \mathbf{Q}_z \tag{17}$$

where $\mathbf{F}$ is a nodal external force vector, and $\mathbf{Q}_z$ is a nodal charge vector in the z direction.

Substituting Eqs. (13)-(17) into Eq. (12) and using Eqs. (1)- (8), we obtain a set of differential equations with respect to x, y and t for the nth element.

$$\mathbf{T}_n = \mathbf{M}_n \ddot{\boldsymbol{\psi}}_n + \mathbf{K}_{Dn} \boldsymbol{\psi}_n \tag{18}$$

where

$$\mathbf{K}_{Dn} = \begin{bmatrix} \mathbf{A}_{Dn} & \mathbf{C}_{Dn} \\ \mathbf{C}_{Dn}^T & -\mathbf{G}_{Dn} \end{bmatrix}, \qquad \mathbf{M}_n = \begin{bmatrix} \mathbf{M}_{sn} & \mathbf{0} \\ \mathbf{0} & \mathbf{0} \end{bmatrix} \tag{19}$$

$$\mathbf{T}_n^T = \{\mathbf{F}_n^T \ \mathbf{Q}_{zn}^T\}, \qquad \boldsymbol{\psi}_n^T = \{\mathbf{d}_n^T \ \boldsymbol{\phi}_n^T\} \tag{20}$$

and

$$\mathbf{A}_{Dn} = -\mathbf{A}_{1n}\frac{\partial^2}{\partial^2 x} - \mathbf{A}_{2n}\frac{\partial^2}{\partial x \partial y} - \mathbf{A}_{3n}\frac{\partial^2}{\partial^2 y} + \mathbf{A}_{4n}\frac{\partial}{\partial x} + \mathbf{A}_{5n}\frac{\partial}{\partial y} + \mathbf{A}_{6n} \tag{21}$$

where the second subscript n denotes the element number. Matrices $\mathbf{C}_{Dn}$ and $\mathbf{G}_{Dn}$ can be expressed in the same way if $\mathbf{A}_{in}$ $(i = 1, \ldots, 6)$ in right hand of Eq. (21) is replaced by $\mathbf{C}_{in}$ and $\mathbf{G}_{in}$, respectively.

Assembling the matrices of all elements, we get the global system differential equations for the whole plate:

$$\mathbf{T}_t = \mathbf{M}_t \ddot{\boldsymbol{\psi}}_t + \mathbf{K}_{Dt} \boldsymbol{\psi}_t \tag{22}$$

where

$$\mathbf{K}_{Dt} = \begin{bmatrix} \mathbf{A}_{Dt} & \mathbf{C}_{Dt} \\ \mathbf{C}_{Dt}^T & -\mathbf{G}_{Dt} \end{bmatrix}, \qquad \mathbf{M}_n = \begin{bmatrix} \mathbf{M}_{st} & \mathbf{0} \\ \mathbf{0} & \mathbf{0} \end{bmatrix} \tag{23}$$

$$\mathbf{T}_t^T = \{\mathbf{F}_t^T \ \mathbf{Q}_{zt}^T\}, \qquad \boldsymbol{\psi}_t^T = \{\mathbf{d}_t^T \ \boldsymbol{\phi}_t^T\} \tag{24}$$

and the subscript t indicates the matrices correspond to the whole plate.

During the process of assembling elements, we make use of the following interface conditions

$$\mathbf{d}_n^u = \mathbf{d}_{n+1}^l \quad \boldsymbol{\varphi}_n^u = \boldsymbol{\varphi}_{n+1}^l \quad \text{for } 1 < n < N-1 \tag{25}$$

in which the subscripts denote the element numbers, and the superscripts denote the lower and upper surfaces of the element.

We introduce the Fourier transformations with respect to the horizontal coordinates x and y as follows:

$$\tilde{\boldsymbol{\psi}}_t(k_x, k_y, t) = \int_{-\infty}^{\infty}\int_{-\infty}^{\infty} \boldsymbol{\psi}_t(x, y, t) e^{-ik_x x} e^{-ik_y y} dx dy \tag{26}$$

where $i = \sqrt{-1}$,and k_x and k_y are the wave numbers for wave propagation in the x and y-axis, respectively. The application of Fourier transformations by Eq. (26) to Eq. (22), leads to the following governing equation in the wave number domain:

$$\tilde{\mathbf{T}}_t = \mathbf{M}_t \ddot{\tilde{\boldsymbol{\psi}}}_t + \mathbf{K}_t \tilde{\boldsymbol{\psi}}_t \tag{27}$$

In this equation, $\tilde{\mathbf{T}}_t$, $\ddot{\tilde{\boldsymbol{\psi}}}_t$ and $\tilde{\boldsymbol{\psi}}_t$ are the transformations of $\mathbf{T}_t$, $\ddot{\boldsymbol{\psi}}_t$ and $\boldsymbol{\psi}_t$, respectively, and $\mathbf{K}_t$ is given by

$$\mathbf{K}_t = \begin{bmatrix} \mathbf{A}_t & \mathbf{C}_t \\ \mathbf{C}_t^T & \mathbf{G}_t \end{bmatrix} \tag{28}$$

where $\mathbf{A}_t$ is the mechanical stiffness matrix given by

$$\mathbf{A}_t = k_x^2 \mathbf{A}_{1t} + k_x k_y \mathbf{A}_{2t} + k_y^2 \mathbf{A}_{3t} + ik_x \mathbf{A}_{4t} + ik_y \mathbf{A}_{5t} + \mathbf{A}_{6t} \tag{29}$$

The piezoelectric coupling matrix, $\mathbf{C}_t$, and dielectric stiffness matrix, $\mathbf{G}_t$, are of the same form as Eq. (29), with $\mathbf{A}$ replaced by $\mathbf{C}$ and $\mathbf{G}$, respectively.

For the eigenvector solution of Eq. (27), the circular frequency for the mth mode can be written in terms of the Rayleigh quotient as

$$\omega_m^2 = \frac{\boldsymbol{\psi}_m^L \mathbf{K}_t \boldsymbol{\psi}_m^R}{\boldsymbol{\psi}_m^L \mathbf{M}_t \boldsymbol{\psi}_m^R} \tag{30}$$

where $\boldsymbol{\psi}_m^L$ and $\boldsymbol{\psi}_m^R$ are the mth transposed left and right eigenvectors.

To visualize the effects of anisotropy on wave propagation, Liu et al. (1991) introduced a set of six characteristic wave surfaces: phase velocity surface (PVS), phase slowness surface (PSS), phase wave surface (PWS),

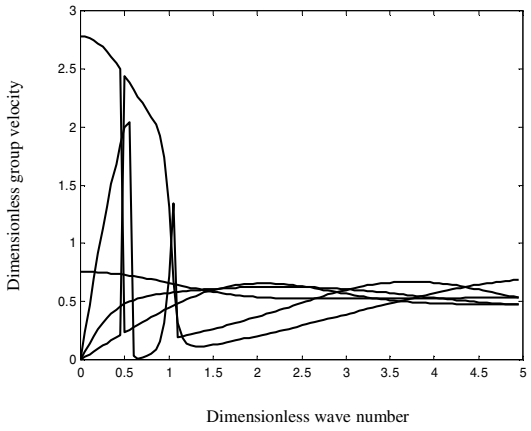

(a)

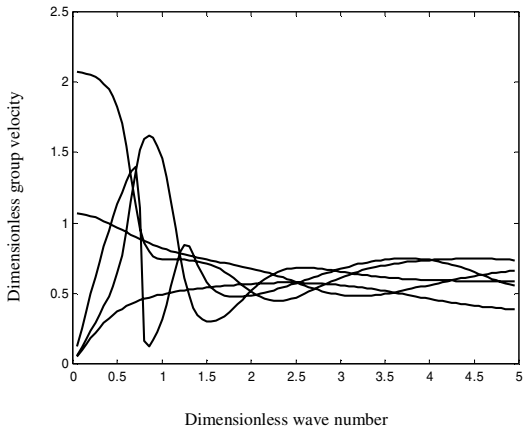

(b)

Figure 2 : Group velocity for wave propagation in the multilayered piezoelectric plate ((a) $\beta = 0^o$; (b) $\beta = 45^o$)

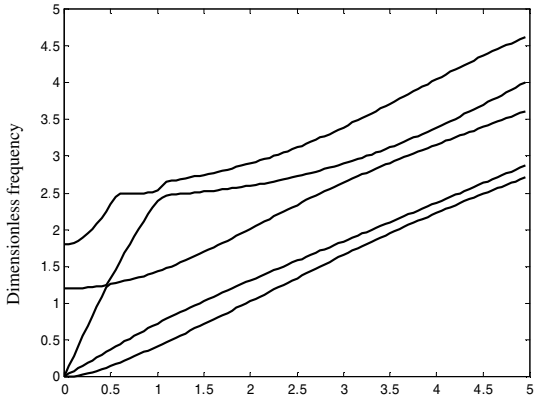

(a)

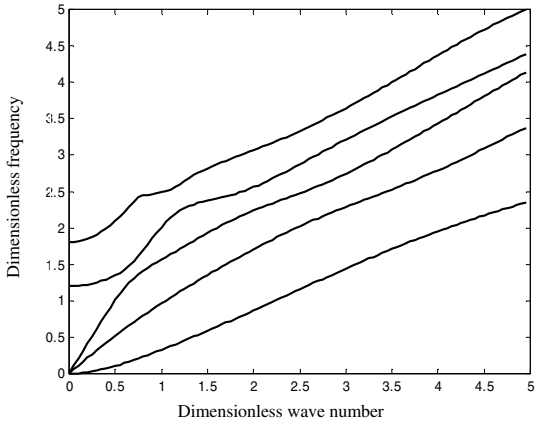

(b)

Figure 3 : Dispersion relationship for wave propagation in the multilayered piezoelectric plate ((a) $\beta = 0^o$; (b) $\beta = 45^o$)

group velocity surface (GVS), group slowness surface (GSS) and group wave surface (GWS). These definitions are adopted here to visualize the characteristic surfaces of waves for the hybrid multilayered piezoelectric laminated plate. The mathematical expressions for these characteristic wave surfaces can be obtained based on the conception of references (Liu et al. (1991); Liu and Xi (2001)).

4 Numerical examples

Based on the foregoing formulation, a FORTRAN program has been developed. In this section, numerical results are presented for the frequency and dispersion relationship as well as characteristic surfaces of waves in the hybrid multilayered piezoelectric laminated plate. The following dimensionless parameters are used:

$$
\begin{aligned}
& c_s = \sqrt{c_{44}^c / \rho_c}\,, \overline{r} = r/H, \\
& \overline{\omega} = \omega H / c_s, \quad \overline{k} = kH, \\
& \overline{\varphi} = \varphi / \varphi_0, \quad \varphi_0 = (e_c f_0 H)/(g_c c_{44}), \\
& e_c = C/m^2, \quad g_c = 10^{-10} F/m
\end{aligned} \tag{31}
$$

where c_{44}^c , ρ_c,e_c and g_c stand for the reference elastic constant, mass density, piezoelectric and dielectrical properties, respectively. In this study, they are taken as the corresponding material properties on the lower sur-

face of the laminate under consideration.

A hybrid multilayered piezoelectric plate with three laminas is studied. Each lamina with same thickness is made of graphite-epoxy, PVDF, and PZT-5A (Vel and Batra 2000; Tang et al., 1996), respectively. Material properties of these three materials are listed in Table 1. In our calculation, each sub-layer is evenly divided into 4 layer elements, as such there are totally 12 layer elements for the entire structure. The piezoelectricity effect is firstly investigated by comparing the natural frequencies of the multilayered plate with or without the piezoelectric material. Their natural frequencies are listed in Table 2. From the table, we can see that the effect of piezoelectricity does not influence the overall shapes of corresponding frequency, but only changes its corresponding values slightly. The change is only occurs at some specified mode.

The computation of group velocity spectra is carried out for the hybrid multilayered piezoelectric plate. Figure 2 illustrates the group velocity spectra for waves propagating in this hybrid multilayered piezoelectric plate. The dispersion of waves in this hybrid multilayered piezoelectric plate is also investigated. Figure 3 illustrates the dispersion curves. The propagation directions of waves are chosen as $\beta = 0^o$, 45^o, respectively. $\beta = 45^o$ is used to show the effect of a wave propagating in any direction. The wave propagation for all the modes in the case of the plate is dispersive. The characteristic surfaces are calculated and the 1^{rd} and 2^{nd} modes are selected and plotted in Figure 4. A full understanding for the complex phenomena of elastic waves in hybrid multilayered piezoelectric media can be clearly drawn from this figure.

5 Conclusions

The frequency and group velocity dispersion behaviors, and characteristic surfaces of waves in hybrid multilayered piezoelectric plate have been investigated. The method of approach is formulated within the framework of the three-dimensional elasticity theory, and is thus accurate in comparison with ones using various plate theories. The coupling between elastic field and the electric field is considered in each element. The characteristic wave surfaces give a full understanding for the complex phenomena of elastic waves in the hybrid multilayered piezoelectric media. The inhomogeneity as well as the anisotropy effect can be observed from these six wave surfaces.

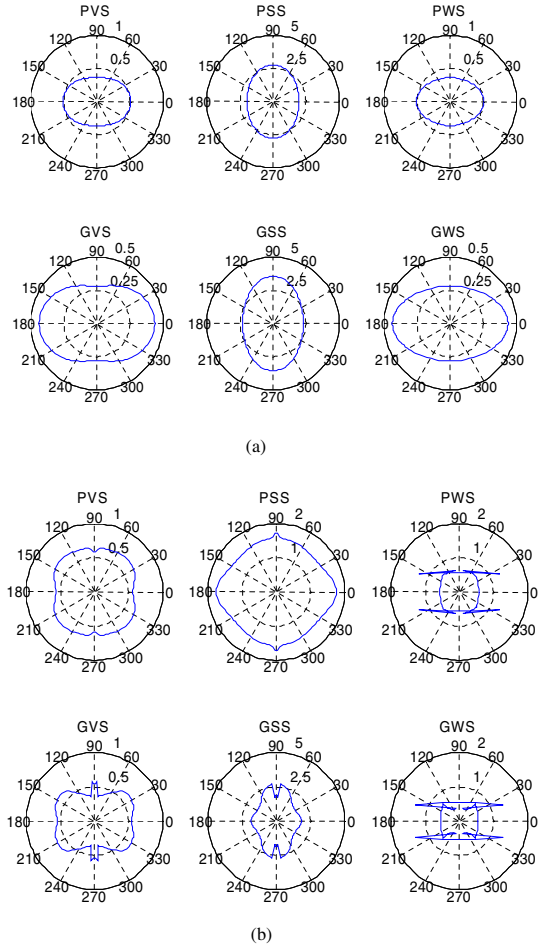

Figure 4 : The characteristic surface for a hybrid multilayered piezoelectric plate ($\overline{k} = 7.78$, (a) 1^{st} mode; (b) 2^{nd} mode

Acknowledgement: This paper has been financially supported by the Special Funds for Major State Basic Research Project under Grant No.2002CB412706; Knowledge Innovation Project of Chinese Academy of Sciences under Grant No.KJCX2-SW-L2.

References

Ericl, Adler (2000): Bulk and surface acoustic waves in anisotropic solids. *International Journal on High Speed Electronics and Systems*, Vol. 10, pp. 653-648.

Bleustein, J.L. (1969): Some simple models of wave propagation in an infinite piezoelectric plates. *J. Acoustic Soc. Am*, Vol. 45, pp. 614-620.

Curtis, R.G.; Redwood, M. (1973): Transverse surface

Table 1 : Material property of the PZT-5A, PVDF and graphite-epoxy

Property	PZT-5A	0^0 PVDF	0^0 Graphite-epoxy
c_{11} (GPa)	99.201	238.2400	183.4430
c_{22} (GPa)	99.201	23.6000	11.6600
c_{33} (GPa)	86.856	10.6400	11.6620
c_{12} (GPa)	54.016	3.9800	4.3630
c_{13} (GPa)	50.778	2.1900	4.3630
c_{23} (GPa)	21.100	1.9200	3.9180
c_{44} (GPa)	21.100	2.1500	2.8700
c_{55} (GPa)	21.100	4.4000	7.1700
c_{66} (GPa)	22.593	6.4300	7.1700
e_{31} (cm^{-2})	-7.209	-0.1300	0.0000
e_{32} (cm^{-2})	-7.209	-0.1450	0.0000
e_{33} (cm^{-2})	15.118	-0.2760	0.0000
e_{24} (cm^{-2})	12.32	-0.0090	0.0000
e_{15} (cm^{-2})	12.322	-0.1350	0.0000
g_{11} ($10^{-10}Fm^{-1}$)	153.000	1.1068	153.0000
g_{22} ($10^{-10}Fm^{-1}$)	153.000	1.1068	153.0000
g_{33} ($10^{-10}Fm^{-1}$)	153.000	1.1068	153.0000

Table 2 : Dimensionless natural frequencies of the lowest six modes for the hybrid multilayered piezoelectric plate with or without piezoelectric property ($\theta = 0$)

$\bar{k}$	piezoelctric	M1	M2	M3	M4	M5	M6
7.78	with	3.968	4.403	5.005	5.896	5.964	6.949
	without	3.962	4.403	5.005	5.896	5.933	6.949
15.62	without	7.456	8.706	9.198	9.640	9.725	10.470
	with	7.444	8.706	9.198	9.632	9.725	10.470

waves in piezoelectric materials carrying a metal layer of finite thickness, *J. Appl. Phys.*, Vol. 44, pp. 2002-2007.

Gopinathan, S.V.; Varadan, V.V.; Varada, V.K. (2000): A review and critique of theories for piezoelectric laminates, *Smart Mater. Struct.*, Vol. 9, pp. 24-48.

Han, X.; Liu, G.R. (2003): Elastic waves in a functionally graded piezoelectric cylinder, *Smart Mater. Struct.*, Vol. 12, pp. 962-971.

Han, X.; Liu, G.R.; Ohyoshi, T. (2004): Dispersion and characteristic surfaces of waves in hybrid multilayered piezoelectric circular cylinders, *Computational Mechanics*, Vol. 33, pp. 334-344.

Honein, B.; Braga, A.M.B.; Herrmann, G. (1991): Wave propagation in piezoelectric layered media with some applications. *Proceedings of the conference on recent advances in active control of sound and vibration*, Technomic.

Lewis, M.F. (1985): On Rayleigh waves and related propagating acoustic waves. In Rayleigh-wave theory and application, Ash, E A and Paige E G S ed. Springer-Verlag.

Liu, G.R.; Dai, K.Y.; Han, X.; Ohyoshi, T. (2003): Dispersion and characteristic wave surfaces in functionally graded piezoelectric plates, *J. Vib and Sound*, Vol. 268, pp. 131-147.

Liu, G.R.; Tani, J.; Ohyoshi, T.; Watanabe, K. (1991): Characteristic wave surfaces in anisotropic laminated plates. *J. Vib. Acoust*, Vol. 113, pp. 279-285.

Liu, G.R.; Tani, J. (1994): Surface waves in functionally gradient piezoelectric plates. *J. Vib. and Acoust*. Vol.

116, pp. 440-448.

Liu, G.R.; Xi, Z.C. (2001): Elastic waves in anisotropic laminates, CRC press.

Liu, J.; Wang, Z.K. (2005): The propagation behavior of love waves in a functionally graded layered piezoelectric structure, *Smart Mater. Struct.*, Vol. 14, pp. 137-146.

Liu, H.; Wang, T.J.; Kuang, Z.B. (2002): Effect of a biasing electric field on the propagation of symmetric waves in piezoelectric plates,*Int. J. Solids Struct.*, Vol. 39, pp. 2031-2049.

Pauley, K.E.; Dong, S.B. (1976): Analysis of plane waves in laminated piezoelectric plates, *Wave Electronics*, Vol. 1, pp. 265-185.

Siao, J.C.T.; Dong, S.B.; Song, J. (1994): Frequency spectra of laminated piezoelectric cylinders, *ASME J. Vib. And Acoust.*, Vol. 116, pp. 364-370.

Shiosai, T.; Mikamura, Y.; Takeda, F.; Kawabata, A. (1986): High-coupling and high-velocity SAW using ZnO and AlN Films on a glass substrate. *IEEE Tran. UFFC*. Vol. 33-3, pp. 324-330.

Sun, C.T.; Cheng, N.C. (1974): Piezoelectric waves on a layered cylinder,*J. Appl. Phys.*, Vol. 23, pp. 83-88.

Tang, Y.Y.; Noor, A.K.; Xu, K. (1996): Assessment of computational models for thermoelectroelastic multilayered plates, *Comput. Struct.*, Vol. 61, pp. 915-933.

Toda, K.; Mizutain, K. (1988): Propagation characteristics of plate waves in a Z-cut X-propagation $LiTaO_3$ thin plate. *Transactions of the institute of electronics, information and communication engineering*, J71-A-6, pp. 1225-1233.

Vel, S.S.; Batra, R.C. (2000): Three-dimensional analysis solution for hybrid multilayered piezoelectric plates, *ASME J. Appl. Mech.*, Vol. 67, pp. 558-567.

Wang, Q. (2001): Wave propagation in a piezoelectric coupled cylindrical membrane shell, *Int. J. Solids Struct.*, Vol. 38, pp. 8207-8218.

Zhang, T.Y.; Qian, C.F.; Tong, P. (1998): Linear electroelastic analysis of a cavity or a crack in a piezoelectric material. *J. Solids Struct.*, Vol. 35, pp. 2121-2149.